Spring 5-2022

Investigating Arrhythmia Potential in Cardiac Myocytes in Presence of Long QT Syndrome

Victoria Lin Lam
Old Dominion University, vlam009@odu.edu

INVESTIGATING ARRHYTHMIA POTENTIAL IN CARDIAC MYOCYTES IN PRESENCE OF LONG QT SYNDROME

by

Victoria Lin Lam
B.S. May 2019, College of William & Mary

A Thesis Submitted to the Faculty of Old Dominion University in Partial Fulfillment of the Requirements for the Degree of

MASTER OF SCIENCE

ENGINEERING - BIOMEDICAL

OLD DOMINION UNIVERSITY
May 2022

ABSTRACT

INVESTIGATING ARRHYTHMIA POTENTIAL IN CARDIAC MYOCYTES IN PRESENCE OF LONG QT SYNDROME

Victoria Lin Lam
Old Dominion University, 2022
Director: Dr. Michel Audette

Long QT Syndrome (LQTS) is an increasingly studied condition that leads to potentially fatal heart rhythm disorders, called arrhythmias, and sudden cardiac death. The alterations in the electrocardiograms (ECGs) seen in LQTS patients is caused by mutations to genes related to ion channels in cardiac cells. Computational modeling allows the mechanistic study of these ion channel mutations in LQTS by providing quantitative predictors of cardiac behavior in human and rabbit heart models. This work hypothesizes that the repolarization reserve in cardiac Purkinje cells (PC), that form the cardiac conduction system, is lower than that of ventricular myocytes (VM), resulting in a higher propensity of electrophysiological abnormalities in the form of spontaneous activity, particularly early and delayed afterdepolarizations (EADs and DADs, respectively). To investigate this hypothesis, detailed computational methods were created by incorporating experimental data. The computer models were then utilized to reproduce the experimentally observed behavior in single cells as well as 3-dimensional ventricular models. The computational results show more profound effects of the LQTS mutations on action potential duration (APD) prolongation in PCs when compared to VMs. Ectopic beats exist in isoproterenol conditions for human PCs. Future research includes determining the effect of these APD differences on the entirety of the heart using an anatomical 3D model of a rabbit heart.

This thesis work is dedicated to my best friends, whose endless supply of support and encouragement during the ups and downs of graduate school kept me afloat. I cannot thank you enough for all you've helped me accomplish. This work is also dedicated to my family, who have always loved me unconditionally and pushed me to achieve my goals.

ACKNOWLEDGMENTS

There are many people who have contributed to the successful completion of this thesis. I extend many thanks to my core research group for their patience and hours of guidance on my research and editing of this manuscript. The untiring efforts of Dr. Michel Audette, Dr. Makarand Deo, Anthony Owusu-Mensah, and Dr. Anna Bulysheva deserve special recognition.

NOMENCLATURE

AP	Action Potential
APD	Action Potential Duration
APD_{50}	Action Potential Duration at 50% Repolarization
APD_{90}	Action Potential Duration at 90% Repolarization
AV	Atrioventricular
ARPF	Aslanidi Rabbit Purkinje Fiber Model
BCL	Basic Cycle Length
Ca^{2+}	Calcium
DAD	Delayed Afterdepolarizations
EAD	Early Afterdepolarizations
ECG	Electrocardiogram
hERG	Human Ether-a-go-go-related Gene
$I_{Ca(L)}$	Long-Lasting Calcium Current
$I_{Ca(T)}$	Transient Calcium Current
I_{K1}	Inward Rectifier Potassium Current
I_{Kr}	Rapid Activating Delayed Rectifier Potassium Current
I_{Ks}	Slowly Activating Delayed Rectifier Potassium Current

I_{To}	Transient Outward Potassium Current
K^+	Potassium
LQT2	Long QT Syndrome Type II
LQTS	Long QT Syndrome
Na^+	Sodium
PC	Purkinje Cell
PMJ	Purkinje Myocardial Junction
PS	His-Purkinje System
SA	Sinoatrial
SCR	Spontaneous Calcium Release
SR	Sarcoplasmic Reticulum
TdP	Torsade de Pointes
VM	Ventricular Myocyte
VT	Ventricular Tachycardia

TABLE OF CONTENTS

Page

LIST OF FIGURES

LIST OF GRAPHS

Graph Page

INTRODUCTION

MOTIVATION

Long QT Syndrome (LQTS), characterized by an abnormally prolonged QT interval on an electrocardiogram (ECG), is listed among life-threatening diseases due to its association with sudden cardiac death [1]. This condition has been increasingly studied in recent years. Prior experimental studies utilizing rabbits and mice have indicated involvement of the His-Purkinje system (PS) on spontaneous polymorphic ventricular tachycardia (VT) and sudden cardiac death in LQTS patients [2], however its exact role remains poorly understood. Computer-based numerical simulations have the potential to provide mechanistic insights into the arrhythmogenic propensity of cardiac PCs.

PROBLEM STATEMENT

Though the connections between the PS and LQTS have been increasingly studied in recent years, the exact influence of potassium channel mutations in electrophysiology of cardiac Purkinje cells (PCs) has not been studied in depth. This research focuses on these potassium channel mutations, particularly in the case of Long QT Syndrome Type II (LQT2), utilizing experimental and computational research. Because LQT2 manifests as VTs, this project focuses on the two primary cell types in ventricles: PCs and ventricular myocytes (VMs) to determine which has more arrhythmia potential. This work hypothesizes that the repolarization reserve in PCs is lower than that in VMs, which lead to more severe LQT2 phenotype in PCs with higher propensity of early (EADs) and delayed afterdepolarizations (DADs).

LITERATURE REVIEW

Four chambers compose the human heart: two atria (top chambers) and two ventricles (bottom chambers). The rhythmic beating of these chambers ensures human survival by providing synchronous blood flow throughout the body. This cardiac rhythm is determined by conduction of electrical action potentials through the heart muscles. The pacemaker, or sinoatrial (SA) node, initiates cardiac impulses, or action potentials (AP). It is located in the right atrium. The electrical signal propagates through atrial tissue, causing contraction of atria, and reaches the atrioventricular (AV) node, which functions to transmit the impulse to the bundle of His and eventually to the ventricles. The AV node also creates a delay in the contraction of the chambers in the heart, allowing a filtering of any atrial tachyarrhythmias. The bundle of His is the only fiber-bundle actually capable of carrying the impulse from the atria to the ventricles via the right and left His bundle branches. The Purkinje fibers are the terminal fibers in this system [3]. They form Purkinje myocardial junctions (PMJ) with VMs. These junctions conduct the cardiac impulse into the myocardium, resulting in proper contraction of the heart under healthy conditions. The basic anatomy of the human heart is shown in Fig. 1.

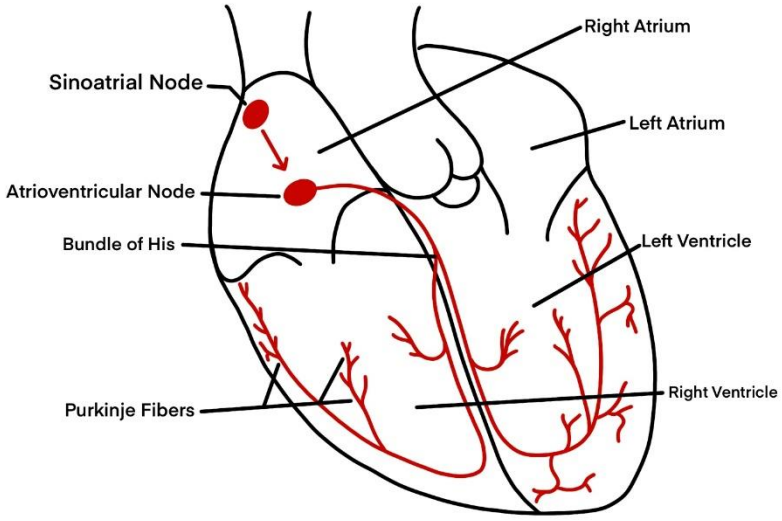

Fig. 1. Basic anatomy of the human heart, including compartments and electrical conduction system.

Movement of ions across the cell membrane through ion channels, pumps and exchangers facilitate the generation of electrical APs in each cardiac cell. Propagating APs through the heart tissue causes the synchronous beating of the heart. A typical cardiac ventricular AP is composed of five phases as shown in Fig. 2. Phase zero is the AP upstroke or rapid depolarization phase, which initiates when a cell reaches the voltage threshold of approximately -65 mV. The inward sodium (Na^+) current (I_{Na}) is the principal ion current responsible for this phase. It is a rapidly activated voltage-dependent channel that is followed by a rapid inactivation, causing a brief rush of I_{Na}. Phase one of the cardiac AP is the early rapid repolarization phase, interrupted when the cell reaches the plateau phase. I_{to}, or the transient outward potassium (K^+) current, provides most of the repolarizing charge in this phase [4].

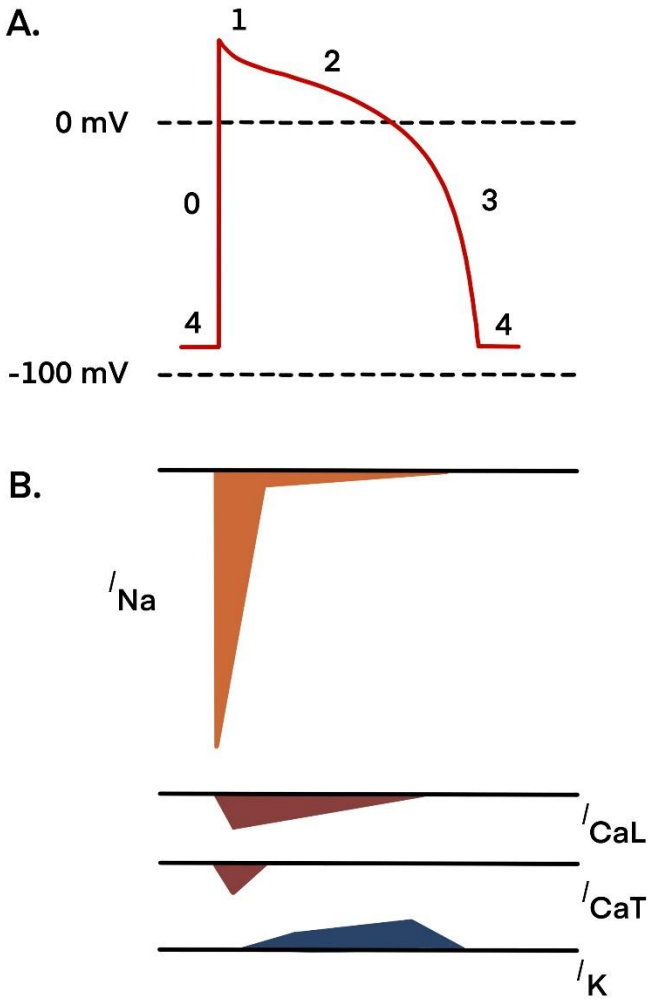

Fig. 2. Plot of cardiac action potential showing main phases (A) and relative influxes and effluxes of main ion currents (B), based off of the information collected in Jalife et al.'s work [4].

During the plateau, or phase two, the cell membrane repolarizes at a much slower rate. The primary acting currents in phase two are the inward calcium (Ca^{2+}) current and the delayed rectifier potassium outward current. There are two primary Ca^{2+} currents: long-lasting calcium current, $I_{Ca(L)}$, and transient calcium current, called $I_{Ca(T)}$. Healthy VMs do not exhibit, $I_{Ca(T)}$, so they rely on $I_{Ca(L)}$ during the plateau phase. PCs have both $I_{Ca(L)}$ and $I_{Ca(T)}$. The K^+ currents

consist of the rapid and slow components, known as I_{Kr} and I_{Ks}, respectively. These channels are activated as the membrane potential becomes more positive than -40 mV, which is reached during the AP upstroke. Ca2+ channels open to allow inward movement of Ca^{2+}, whereas the K^+ ions move outward as indicated in panel B of Fig. 2. The Ca^{2+} current acts as a depolarizing force, but the outward movement of K^+ ions negate the force of the of the Ca^{2+} ions. The balance between the Ca^{2+} and K^+ currents determine the membrane potential in phase two. The plateau phase ends when Ca^{2+} channels are inactivated, but the potassium channels are still open, enabling rapid repolarization of the membrane towards its resting state [4].

This brings about phase three: final repolarization. This phase is driven by the inward potassium current, I_{K1}, as I_{Kr} and I_{Ks} channels tend to close as the cell repolarizes, particularly when it reaches a membrane potential around -40 mV. I_{K1} also helps to set the resting potential of cardiac cells. Compared to nodal cells, PCs and VMs have different resting membrane potentials, which can be explained by the presence of I_{K1} in these cardiac cells but less so in nodal cells. Phase four is the resting membrane potential, which sits at about -90 mV [4].

Though the morphological structure of the PS is well-studied and characterized, PMJs are less understood. In 2017, Garcia et al. analyzed several properties of PMJs, including PMJ density in various heart regions, in porcine hearts utilizing tissue samples. Their study indicates that PCs are less densely packed in the base versus the middle third and apex of the heart [5]. PMJs function through gap junctions with a connexin subunit, which plays a role in the conduction of the cardiac impulse from the PS to VMs, and vice-versa. Olejnickova et al.'s work furthers the understanding of ventricular activation via PMJs in healthy hearts through their investigation of connexin subunit of gap junctions and the role it plays in the activation pattern of the ventricles [6].

Patients suffering from acquired or congenital LQTS, have an abnormally lengthened ventricular repolarization as shown in Fig. 3. This lengthening causes VTs and even sudden cardiac death, particularly when under stress. To reiterate, VMs do not spontaneously elicit APs; they require excitation from the PS, or from neighboring activated myocytes. The lengthening of the ventricular repolarization, shown in the form of a prolonged QT interval on ECGs, may initiate arrhythmias due to temporary conduction blocks in partially-excitable ventricles during the propagation of sinus beats emitted by the PS. The ventricles have a refractory period that prevents conducting new beats immediately after previous activation, but these conduction blocks may precipitate the formation of re-entry, which can eventually lead to arrhythmias. LQT2, accounting for 35–40% of all LQTS patients, is characterized by a mutation of the human ether-a-go-go-related gene (*hERG*) gene. This gene is principally responsible for encoding the pore-forming unit of the rapid activating delayed rectifier potassium channels. These channels control the rapid activating delayed rectifier current, I_{Kr}, which is critical in regulating cardiac AP repolarization. The modification of this gene results in a reduction or complete inhibition of I_{Kr}, prolonging the QT interval and lengthening action potential duration (APD) [1].

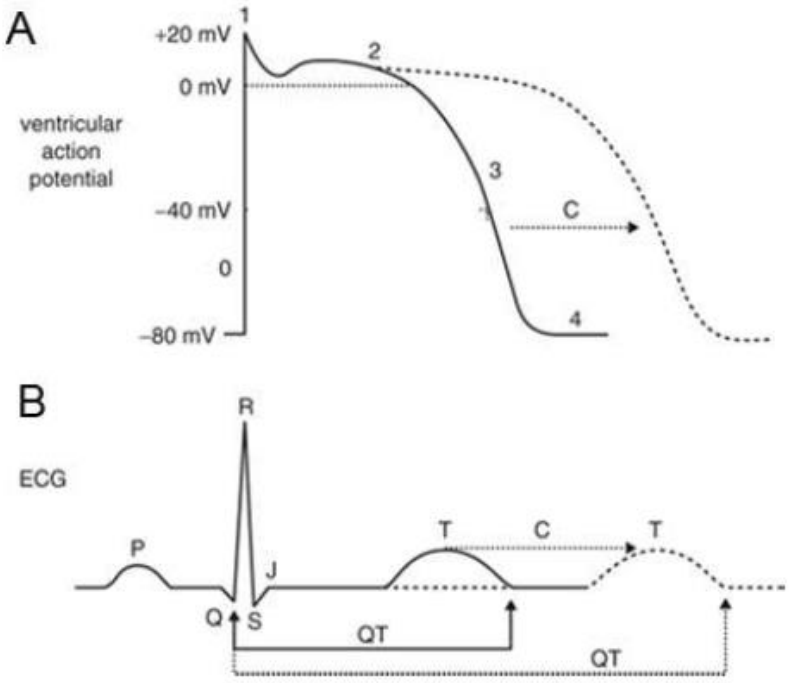

Fig. 3. APD prolongation (A) leading to Long QT morphology as seen in ECG (B).

In LQTS patients, a morphological difference presents itself in the ventricular repolarization; the T-waves have a higher prevalence of being biphasic, meaning that the wave has two distinct components of opposite polarity, or notched, when a second positive deflection occurs [7]. These can both be related to formation of EADs. A comparison between a biphasic and normal, or monophasic, T-wave is shown in Fig. 4. EADs have been found to propagate under LQT2 conditions [8]. Due to the advances in understanding of the molecular basis of this disease, perhaps the most promising treatment method is that of gene-based therapeutic approaches [1]. If all molecular phenotypes of LQT2 are studied and properly understood, the chance of creating a gene therapy for the syndrome will greatly increase. Though it is known that a reduction in I_{Kr} causes the QT prolongation, the effects of these mutations specifically in PCs is

not well-understood and requires further investigation, especially including the role of the repolarization reserve of PCs versus VMs. Studies involving the repolarization reserve indicate that when one repolarizing current is blocked, the other repolarizing currents will try to compensate for the loss. In the case of cardiac cells under LQTS conditions, the loss of I_{Kr} is replaced by I_{Ks} in some capacity. In PCs, I_{Ks} does not play as much of a role as I_{Kr}, so the repolarization reserve is weaker than that of VMs. This leads to worsened APD prolongation, which may lead to spontaneous cardiac activity, like EADs and DADs [9]. EADs and DADs are different morphologically, as depicted by Fig. 5; EADs occur before the AP has fully repolarized, whereas DADs occur following the complete repolarization of the AP.

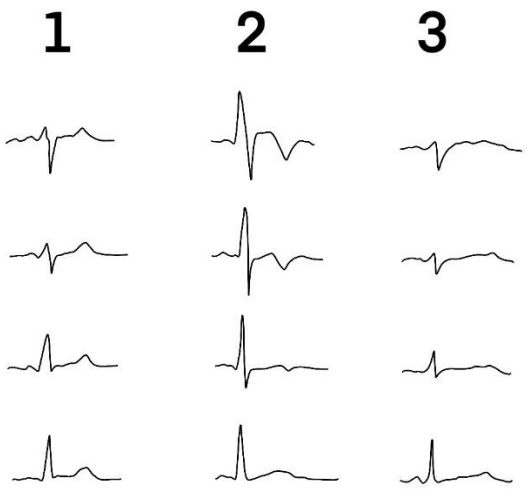

Fig. 4. Examples of T wave patterns. Column 1 corresponds to a normal T wave, Column 2 corresponds to a biphasic T wave, and Column 3 corresponds to a notched T wave where the notch is identified by an arrow [7].

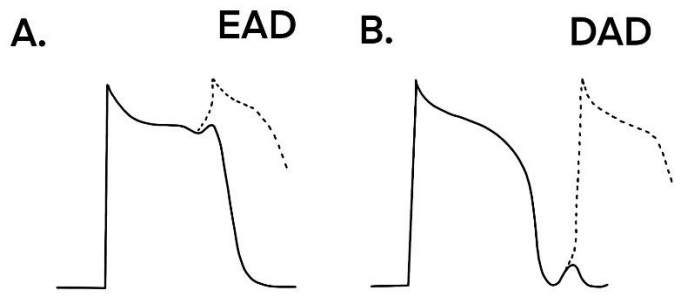

Fig. 5. Comparison between EADs (A) and DADs (B).

In order to investigate the role that PCs play in LQTS or any cardiac condition, computational biophysical models of hearts can be used by replicating results seen in vivo and predicting how the heart may react under abnormal conditions. These models are particularly useful when in vivo studies are difficult to conduct. Hodgkin and Huxley provided the first computational model of an AP in the 1950s, establishing a still-used basis for many electrophysiological models. Their model shows that inward sodium (Na+) movement depolarizes the AP to a peak amplitude around 40 millivolts. An outward potassium (K+) movement repolarizes the membrane potential, temporarily hyperpolarizing the membrane before it returns to its resting potential around -70 millivolts. These preliminary findings led to the question of whether a mathematical model based on these findings could be used to reproduce the experimentally-determined AP morphology. Ultimately, Hodgkin and Huxley successfully reproduced the APs in their model. Eq. 1 outlines the reversal potential as defined by Hodgkin and Huxley, which takes into account the interactions of various ion currents in the cell [10].

$$I = C_m \frac{dV_m}{dt} + g_K(V_m - V_K) + g_{Na}(V_m - V_{Na}) + g_t(V_m - V_i) \qquad \textit{Eq. 1}$$

Though Hodgkin and Huxley were the first to computationally reproduce APs, cardiac APs were not modeled until the 1970s. Their work served as the basis for these models, particularly regarding the formulation of ionic currents, but these models needed to include Ca^{2+} intake through $I_{Ca(L)}$ channel release. This channel is present in the cells of the myocardium, but not included in the Hodgkin-Huxley formulation. This current triggers calcium-induced calcium-release mechanism, where small amount of Ca^{2+} influx through Ca^{2+} channels activate much larger release of Ca^{2+} stored in the sarcoplasmic reticulum (SR). Properly formulating this mechanism was necessary to reproducing cardiac APs, which was done by Beeler and Reuter in 1977. The structure and kinetics of cardiac ion channels were then expanded upon and represented by mathematical formulas [10].

Studying and understanding these components led to computational cardiac models, that of humans and animals. Since ethical limitations prevent the study of human conditions in human participants, particularly in cases such as LQTS where inducing a phenotype could result in death, animal models are commonly used experimentally. To build on these studies, models of animal hearts are often used to indicate what may be happening in the human condition as well. Of course, the outputs of these animal models must be compared to that of humans to ensure that the results are similar enough to extrapolate their findings and support hypotheses in the human subject. In a quantitative comparison of human and nonhuman cardiac ventricular electrophysiology utilizing computational models, O'Hara and Rudy [11] suggest that species differences potentially cause differences in arrhythmic behavior and drug response. In particular, they find that I_{Kr} has a stronger effect on AP prolongation in humans than in dogs or guinea pigs.

These differences suggest that animal models may be used, but ultimately human models are the most accurate way to validate computational findings [11]. In order for these computational models to be used as quantitative predictors, researchers should often calibrate them to ensure that they are producing physiological results when under normal conditions [12].

Though creating a stable model produces a usable predictor for normal conditions, sometimes this stability entails limitations when studying abnormal hearts. In order to create the EADs and DADs seen in LQT2, the model cannot be entirely stable; the electrotonic loading effect produced at the junction between the PCs and the VMs suppresses the spontaneous activity. In order to combat this, the heart model must be calibrated or modified to fit the needs of the researchers. The work of Campos et al. suggests that increasing Ca^{2+} release from the sarcoplasmic reticulum (SR) and flooding the cell, replicating the effects of abnormal Ca^{2+} cycling, will trigger $I_{Ca(L)}$ and cause spontaneous Ca^{2+} release (SCR). SCRs will stimulate inward currents sensitive to Ca^{2+}, generating spontaneous activity in an anatomically accurate computer model of a rabbit heart [13]. Further research supports the notion that SCR leads to arrhythmia-causing spontaneous activity [14]. This type of activity must be reproducible in a computational model in order to fully investigate the effects of LQT2 on the propagation of spontaneous activity across PMJs.

METHODOLOGY

EXPERIMENTAL METHODS

The experimental component of this research consisted of tissue-level, or whole heart, experiments. The experiments were completed in the Masonic Medical Research Institute, an American Association for Accreditation of Laboratory Animal Care, international accredited facility, which utilizes an Institutional Animal Care and Use Committee approved protocol to perform experiments on male or female New Zealand White Rabbits weighing between 2.8 and 3.2 Kg. The rabbits were deeply anesthetized with ketamine/xylazine (35/5 mg/kg), and then a sternotomy was quickly performed using a scalpel to expose the heart [15]. The heart was excised using scissors by severing the ascending aorta, vena cava, pulmonary vessels, and attached interstitial connective tissue, esophagus, and trachea, effectively completing euthanasia. The heart was placed in a cardioplegic solution consisting of 4 degrees Celsius Tyrode's solution, which was roughly isotonic with interstitial fluid, containing 12 mM of Potassium. The complete contents of the Tyrode's solution were as follows: 129mM NaCl, 20mM $NaHCO_3$, 5.5mM D-Glucose, 0.9mM NaH_2PO_4, 5mM $MgSO_4$, 4mM KCL, and 1.8mM $CaCl_2$.

The rabbit hearts were trimmed, removing unwanted tissue like fat. A dissecting scope was used to locate the fat and other unwanted components. The ventricle was then split to allow visualization of the inner ventricular surface. After trimming the heart, a segment of the cardiac tissue was removed and placed into the apparatus shown in Fig. 6. Tyrode's solution was used throughout the entire experiment to maintain tissue viability. This solution was bubbled/oxygenated with a mixture of 95% O_2 + 5% CO_2 to maintain a constant 7.4 pH for the

experiment. The Tyrode solution was super-fused to the preparation at a pump speed to maintain a constant temperature of 37 degrees Celsius.

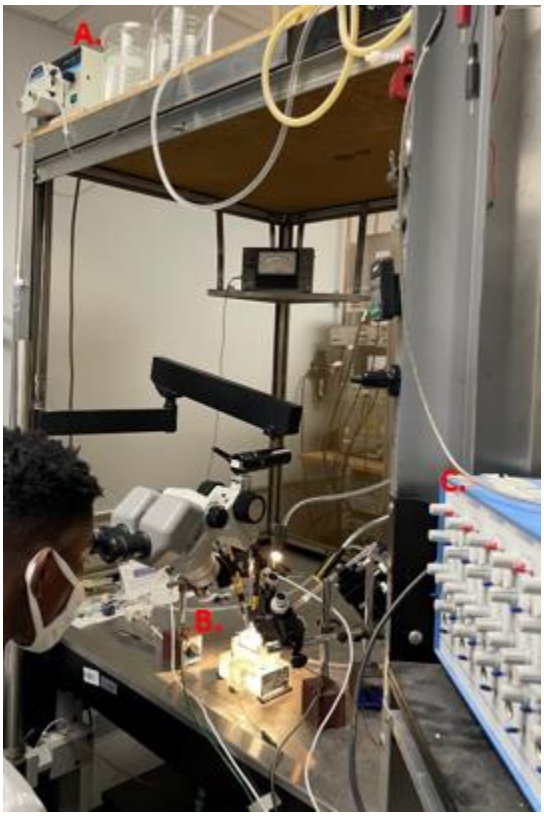

Fig. 6. Experimental setup pumping bubbled Tyrode's solution (A) to chamber (B) containing rabbit heart tissue and stimulating the tissue through a stimulator (C).

The free running Purkinje fibers and ventricular myocardium were initially paced with field stimulating silver-chloride wires across the chamber via a Frederick Haer Pulsar 6i stimulator in normal mode at approximately 20-30 volt at a basic cycle length of 600 ms, which corresponds to about 1.67 Hz, and allowed to recover post-surgery for a time to be determined by

tissue recovery. After recovering, all control and experimental APs were then recorded via bi-polar electrode stimulation with direct contact on the preparation with 3-4 volt/5msec pulse duration stimulation using the basic cycle length (BCL) of 1,000 ms and 500 ms. These BCLs, which correspond to 1 and 2 Hz pacing, respectively, were used to follow the methods of prior studies [13]. Intracellular signals were recorded via glass microelectrode filled with a 2.7M KCl solution with a glass resistance of 20-25 MΩ. These outputs were monitored for APD prolongation as well as any spontaneous activity in the forms of EADs or DADs using a CED 1401 Amplifier utilizing Spike Version 2 Version 7.12 and 2 WPI Model 705 Electrometers for microelectrode recordings. Unfortunately, due to experimental limitations and difficulties in maintaining a consistent distance between the electrodes, the distance between the electrodes was not standardized.

The control data was recorded in the tissue submerged in Tyrode's solution prior to any exposure to drugs. The experimental groups consist of the same tissue after exposure to the drug, E-4031. E-4031 is commonly used to block I_{Kr} in vitro [15]. This drug essentially induces LQT2 conditions by blocking HERG channels. The E-4031 concentrations were varied from 0.1μM to 0.5μM to study dose-dependent I_{Kr} -blockage effects.

SINGLE CELL SIMULATIONS

This work used previously published rabbit models developed by Mahajan et al., to simulate rabbit VM [16], and Aslanidi et al. model of a rabbit PC [17]. Prior ventricular models were developed to represent physiologic heart rates, but they did not accurately depict rapid heart rates, which occur during tachyarrhythmias. These models neglected intracellular Ca^{2+} transient

alternans during rapid pacing, which was seen experimentally and believed to play a role in arrhythmogenesis [16].

To address these limitations, Mahajan et al. modified a previously described rabbit VM model [18] by utilizing a Markovian formulation of $I_{Ca(L)}$, which plays a key role in intracellular Ca^{2+} cycling and regulation of the slope of APD restitution, and by modifying the intracellular Ca^{2+} cycling component itself by incorporating a model that produces the required instability to generate alternans. The first modification was accomplished by using experiments to characterize I_{CaL} in rabbit VMs using patch-clamping. This data was incorporated into a seven-state Markovian model of the current, using voltage-dependent inactivation and calcium-dependent inactivation. The second modification was done using an intracellular Ca^{2+} cycling model previously described and then modified to replicate the desired alternans [18].

Campos et al.'s model for the rabbit VM was also used as a comparison to the Mahajan et al. model in presence of spontaneous Ca^{2+} leaks from SR. Campos et al. sought to investigate the link between SCRs and premature ventricular complexes by seeing what conditions DADs can overcome electrotonic loading. To add this component of SCR, an experimentally based model of SCR was coupled to the Mahajan-Shiferaw model. They doubled the strength of the Na^{+}/Ca^{2+} exchanger and decreased the inward rectifier potassium current to 30% of its control value based on experimental evidence showing this electrophysiological remodeling under pathologies such as heart failure where the propensity for DADs is increased [13].

In 2010, Aslanidi et al developed the Aslanidi Rabbit Purkinje Fiber, (ARPF) model to describe the rabbit PC. Prior to their work, the different ionic mechanisms in PCs versus VMs were not characterized systematically. Similar to Mahajan et al., this model is also based on the Shannon et al. formulations, modified to incorporate experimentally recorded differences in ionic

channel properties between PCs and VMs. The specific changes that were made were the conductance of the fast sodium current was 2.5x greater than the original model, the late sodium current was 10x larger, the conductance of $I_{Ca(L)}$ was increased by 10%, $I_{Ca(T)}$ was added, the conductance of I_{to} modified to fit steady-state inactivation curves, the conductance of I_{Ks} was down modulated, and I_{K1} parameters were modified. The conductance of I_{Na} was multiplied by 2.5 because it matched the AP upstroke velocity of experimental measurements. The late Na current was multiplied by 10 because experimental findings showed that it is significantly larger in PCs than VMs. The conductance of $I_{Ca(L)}$ was increased by 10% to account for differences in current density observed among different cell types. $I_{Ca(T)}$ was added as it is not present in VMs. The conductance of I_{Ks} was decreased because I_{Ks} is smaller in PCs than VMs. Finally, the conductance of I_{K1} was modified based on different resting membrane potentials of cell types [17].

To simulate human cardiac cells, Tusscher et al. model of a VM [19] was used as well as Stewart et al.'s model of the human PC [20]. Tusscher et al. model utilizes experimental data the fast sodium, L-type calcium, transient outward, rapid and slow delayed rectifier, and inward rectifier currents recorded in healthy human VMs. Their model also incorporated basic Ca^{2+} dynamics. As with the other models, the cell membrane was modeled as a capacitor connected in parallel with variable resistances and batteries representing the different ionic currents and pumps. The electrophysiological behavior of a single cell can hence be described with the following differential equation shown below,

$$\frac{dV}{dt} = \frac{I_{ion}+I_{stim}}{C_m} \qquad \textit{Eq. 2}$$

where V is voltage, t represents time, I_{ion} stands the sum of all transmembrane ionic currents as described by the below equation, I_{stim} is the externally applied stimulus current, and C_m is cell capacitance per unit surface area [19].

$$I_{ion} = I_{Na} + I_{K1} + I_{to} + I_{Kr} + I_{Ks} + I_{CaL} + I_{NaCa} + I_{NaK} + I_{pCa} + I_{pK} + I_{bCa} + I_{bNa} \quad \textit{Eq. 3}$$

In 2009, Stewart et al. modified the Tusscher et al. VM model based off experimental data collected in 2002 of Purkinje fibers. They added two currents to the TT2 model: a hyperpolarization-activated or funny current, I_f and a sustained potassium current, I_{sus}. The resultant I_{ion} is shown below.

$$I_{ion} = I_{Kr} + I_{Ks} + I_{K1} + I_{to} + I_{sus} + I_{Na} + I_{b,Na} + I_{Ca,L} + I_{b,Ca} + I_{NaK} + I_{NaCa} + I_{p,Ca} + I_{p,K} + I_f \quad \textit{Eq. 4}$$

The researchers also reformulated I_{K1} and I_{to} as well as altering the maximum conductance of the rapid and slow delayed rectifier potassium currents and the fast sodium current due to differences in the channel kinetics and current densities between PCs and VMs. More specifically, I_{to} is smaller in PCs, but I_{sus} is significantly larger in PCs. The funny current is believed to influence spontaneous diastolic depolarizations, causing automaticity in PCs. This

current was added to the model using equations and parameters that were validated by simulated funny currents during patch clamp experiments. I_{K1} has a much smaller density in PCs than VMs in rabbit hearts, so that is why I_{K1} was reformulated in this model [20].

The single-cell simulations were performed using OpenCARP, which is an open-source cardiac electrophysiology simulator for in-silico experiments [21]. Being open-source, it allows students and researchers to access pre-coded biophysical models that have been added to the repository. The simulations were run on Old Dominion University's (ODU) high performance computing (HPC) clusters. All parameters were modified using Python scripts. Single cell simulations were able to be run directly in the terminal, and all files were transferred to the local drive for analysis utilizing WinSCP. The output files were analyzed and visualized using MATLAB.

The computer simulations were run systematically, completing the same simulations in all four of the above models. The first set of simulations were run at a standard pace of a BCL of 400 ms in the rabbit models as determined by prior literature [13]. A BCL of 1000 ms was used in the human models to allow for complete repolarization of the AP after each stimulus. The first set of simulations was conducted with no alterations in the model parameters, except that the human PC model's Na+ funny current was reduced by 50% to remove automaticity. Then, an analysis of varied I_{Kr} blockage was conducted to try and establish a standard as to what dosage of E-4031 relates to what percent I_{Kr} blockage. I_{Kr} was blocked at 50%, 75%, and 100% by adjusting the conductance of I_{Kr} in each model. The next set of simulations involved 0, 50, 70, and 100% I_{Kr} blockage with isoproterenol conditions which mimic adrenergic stimulation. These were compared to the runs without isoproterenol conditions to provide a comparison of LQT2 with and without stress. In order to simulate isoproterenol conditions, the conductance of I_{Ca} was

increased by 200%, the conductance of I_{K1} is decreased by 20%, and the activity of the Na^+/K^+ pump is increased by 135% [22] with a pacing of 400 BCL to match the control conditions of prior research [13].

Pacing was then varied in both the 0 and 100% I_{Kr} blockage situations, as pacing can sometimes have an effect in the APD restitution or repolarization. The outputs of the VM and PC models in both the rabbit and human scenario were then compared against their own cell type in the opposing species as well as the opposite cell type in the same species. In the human PC model, the sodium funny current was reduced by 50% to prevent spontaneous APs under control conditions.

RESULTS

RABBIT PURKINJE CELLS VERSUS VENTRICULAR MYOCYTES

In the experimental study of the rabbit myocardium, the voltage versus time plot reveals that Purkinje fibers have a 18.7% increase in APD_{50} under the 0.1 uM E-4031 condition and 93.0% increase under the 0.5 uM E-4031 condition, whereas the ventricular myocardium have a 15.8% and 30.1% increase in APD_{50} under the 0.1 uM E-4031 and 0.5 uM E-4031 conditions, respectively. PCs have a 0.881% increase in APD_{90} under the 0.1 uM E-4031 condition and 48.8% increase under the 0.5 uM E-4031 condition, whereas the VMs have a 10.5% and 43.2% increase in APD_{90} under the 0.1 uM E-4031 and 0.5 uM E-4031 conditions, respectively. This is shown in Fig. 7 (A). Fig. 7 (B) and (C) show plots of the drug concentration versus APD in both APD_{50} and APD_{90} scenarios. A two-way ANOVA test was run to determine if there is an interaction between the drug concentration and the APD_{50} and APD_{90} values in the PC versus VM. For the APD_{50}, the p-value was below 0.5, so the null hypothesis that the concentration of E-4031 has no effect on APD_{50} prolongation could not be rejected in either drug concentration. For APD_{90} and 0.5 uM E-4031 conditions, however, the null hypothesis could be rejected as the p-value was 0.02112. Essentially, the significance here is that APD_{90} shows a significant difference in the PCs versus the VMs in the presence of the I_{Kr} blocker, E-4031 at a concentration of 0.5 uM.

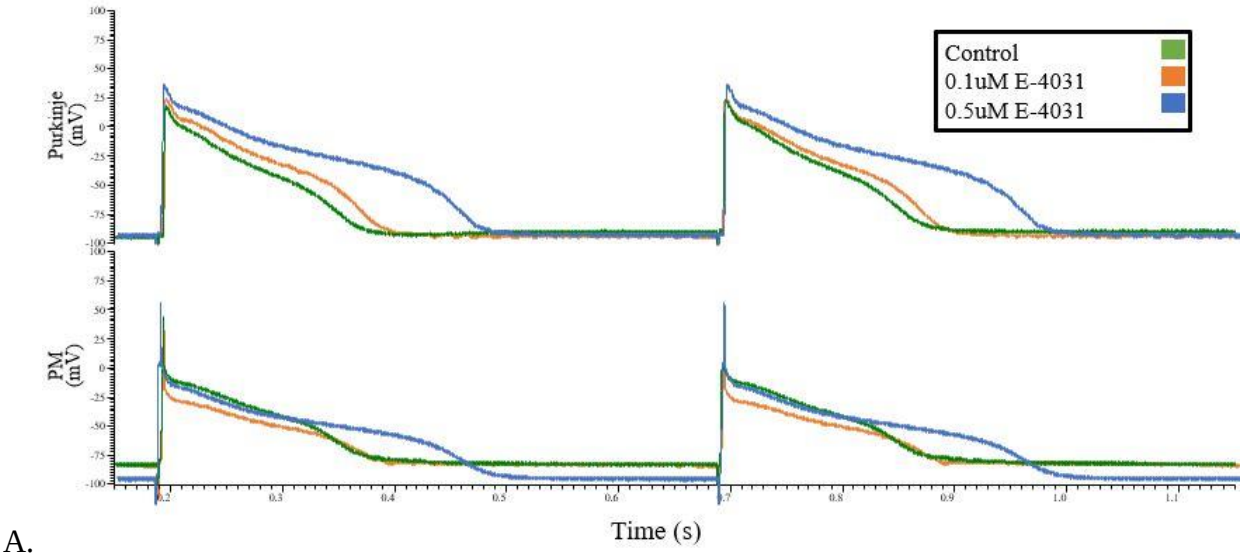

A.

B.

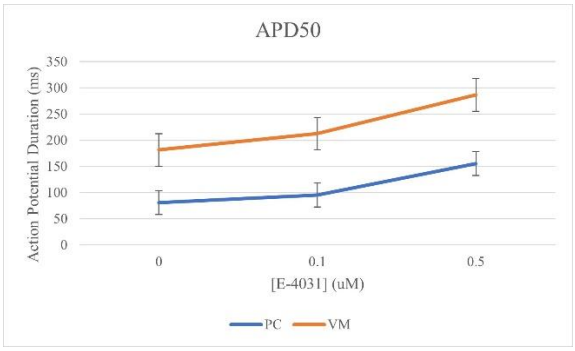

C.

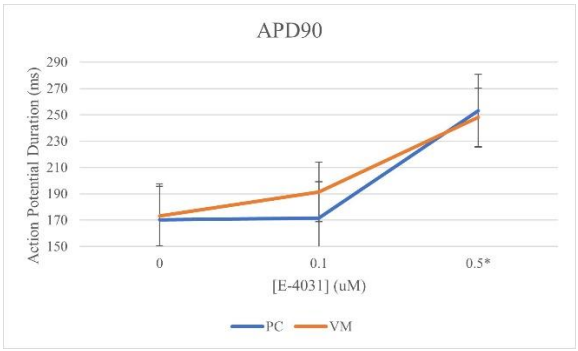

Fig. 7. Voltage versus time plots in PCs and Papillary Muscle (to be compared to VMs) under control, 0.1 uM E-4031, and 0.5 uM E-4031 conditions (A). Plot of APD_{50} (B) and APD_{90}* (C) values in rabbit PCs and VMs.

* Indicates statistical significance

In the computational rabbit models, systematic analysis of the results firstly show that the control models accurately depict the differences between AP morphologies of VMs and PCs shown in experiments, with their respective plateau phases occurring near 0 mV and -30 mV as

shown in Fig. 8. I_{Kr} blockage results in a more pronounced APD prolongation in PCs than VMs. In addition, DADs occur in presence of I_{Kr} blockage in PCs, but not in VMs, as shown in Fig. 8 (B and C). As per Graph 1, the blockage of I_{Kr} results in a greater magnitude of I_{Ks} transients, indicating the influence of a greater repolarization reserve in PCs than VMs as will be investigated in greater detail in the discussion.

A.

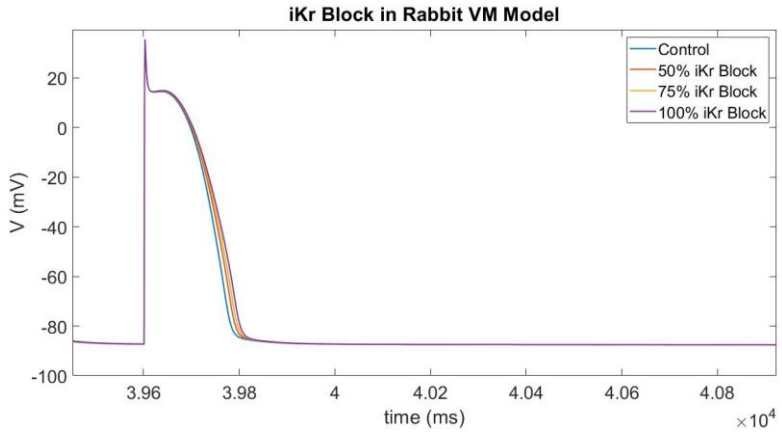

B.

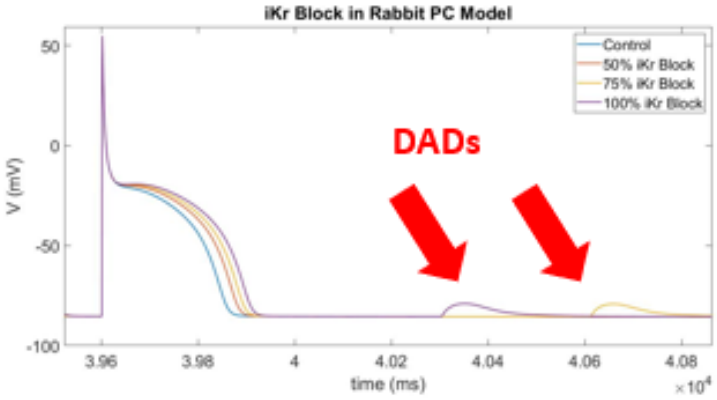

C.

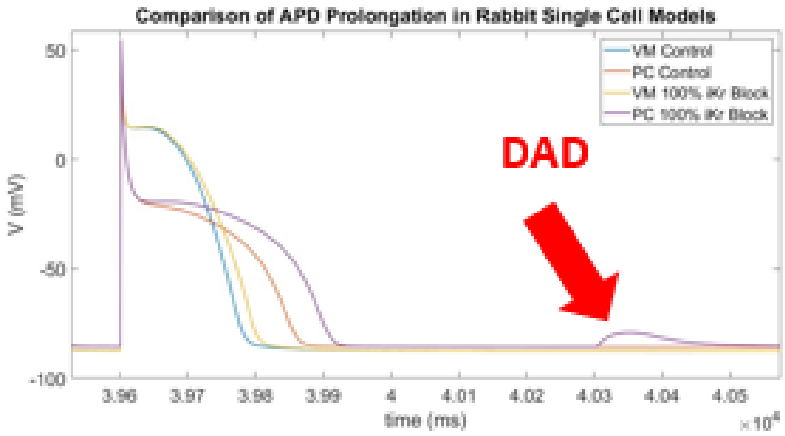

Fig. 8. Comparison of varied levels of I_{Kr} blockage in rabbit VM (A) and PC (B) models. Comparison of 0 versus 100% I_{Kr} blockage in rabbit VM and PC models (C). DADs are present in the presence of I_{Kr} blockage.

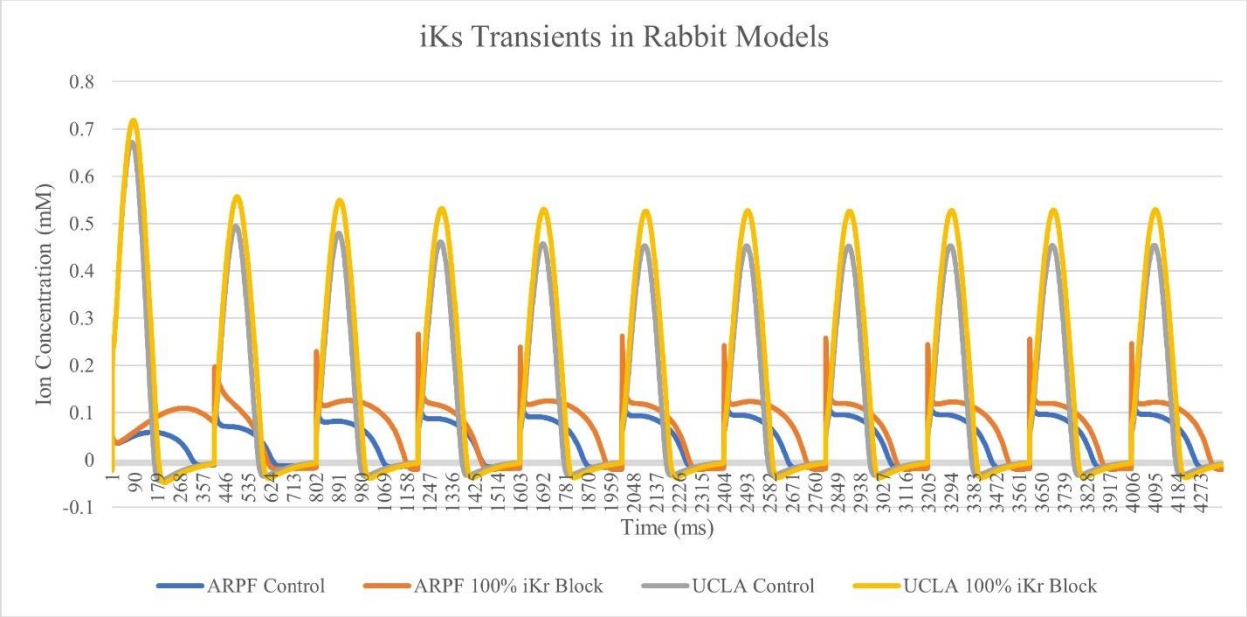

Graph 1. Plot of I_{Ks} transients over time for the rabbit PC and VM models. This indicates that under I_{Kr} block conditions, I_{Ks} must compensate for the missing repolarizing current. VMs appear to have a greater increase in I_{Ks} transients with I_{Kr} blockage.

Under isoproterenol conditions, the rabbit VM and PC models did not produce any DADs, but a more pronounced APD prolongation is present. The AP morphology is altered as well under isoproterenol conditions, particularly in the PC model, as shown in Fig. 9. With varied pacing, increasing the basic cycle length (BCL) produces very little effect in the control simulations, but it produces a slight APD prolongation in both VMs and PCs under I_{Kr} block conditions. These results are reflected in Fig. 10.

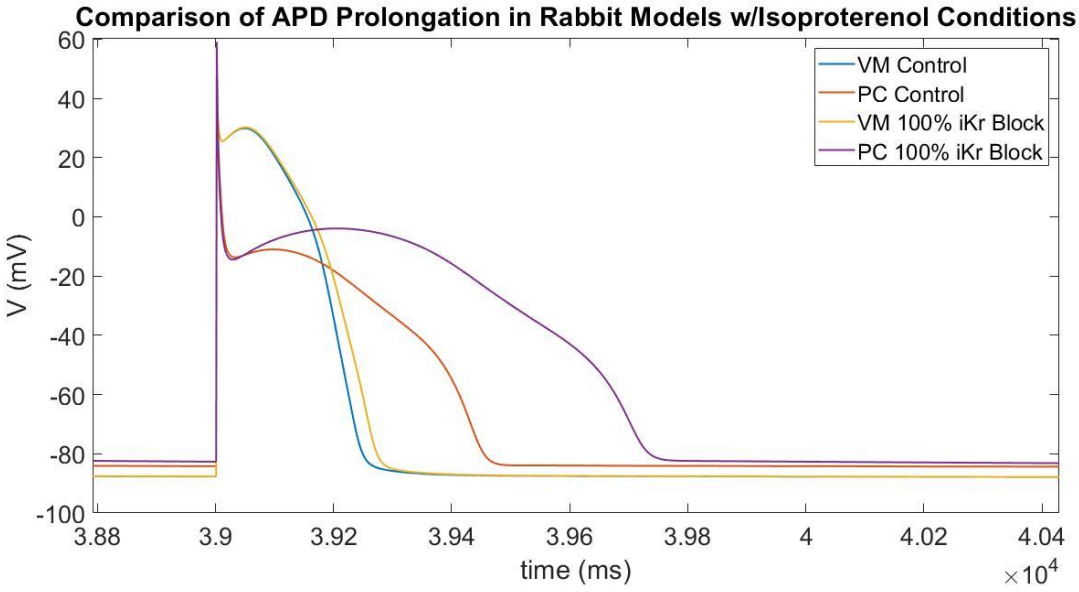

Fig. 9. Comparison of APD prolongation in rabbit models with isoproterenol conditions.

A.

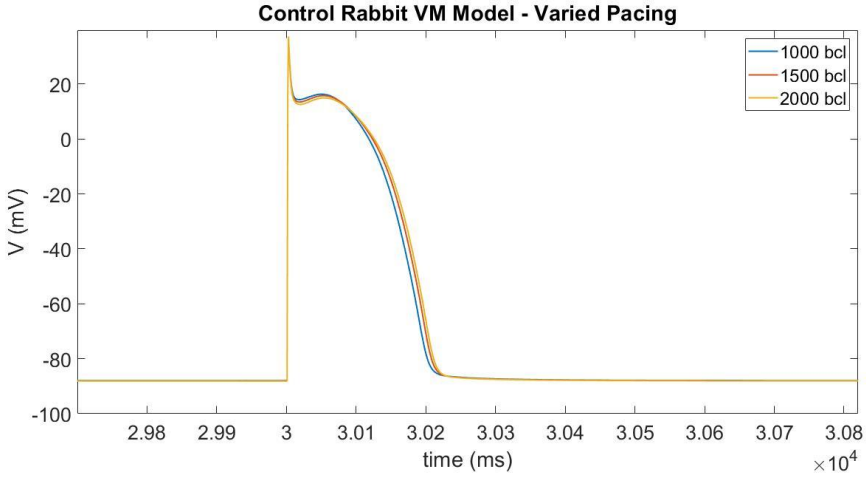

B.

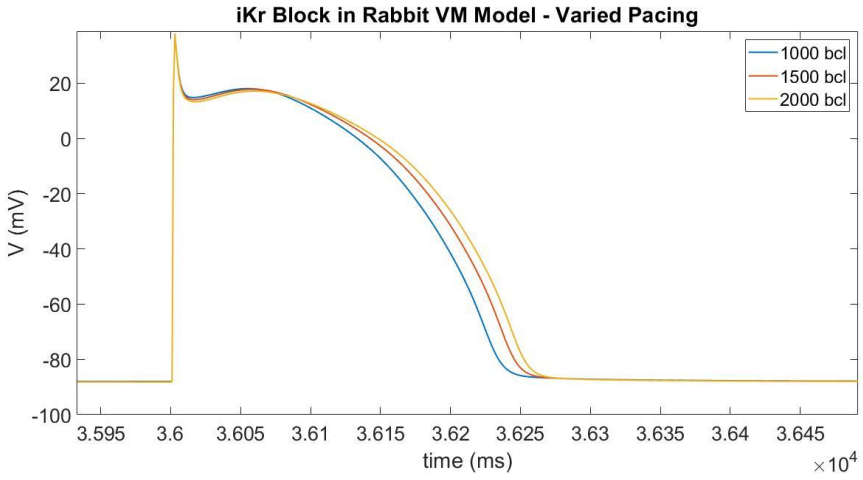
iKr Block in Rabbit VM Model - Varied Pacing
1000 bcl
1500 bcl
2000 bcl
V (mV)
time (ms)
×10^4

C.

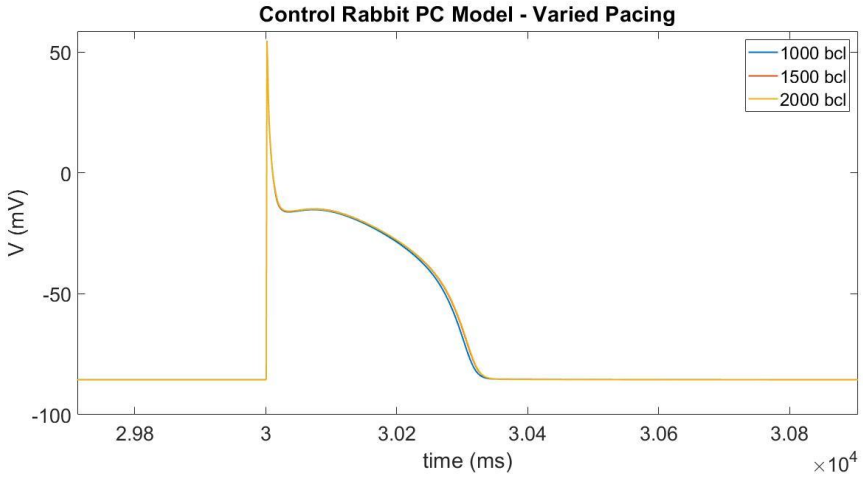
Control Rabbit PC Model - Varied Pacing
1000 bcl
1500 bcl
2000 bcl
V (mV)
time (ms)
×10^4

D.

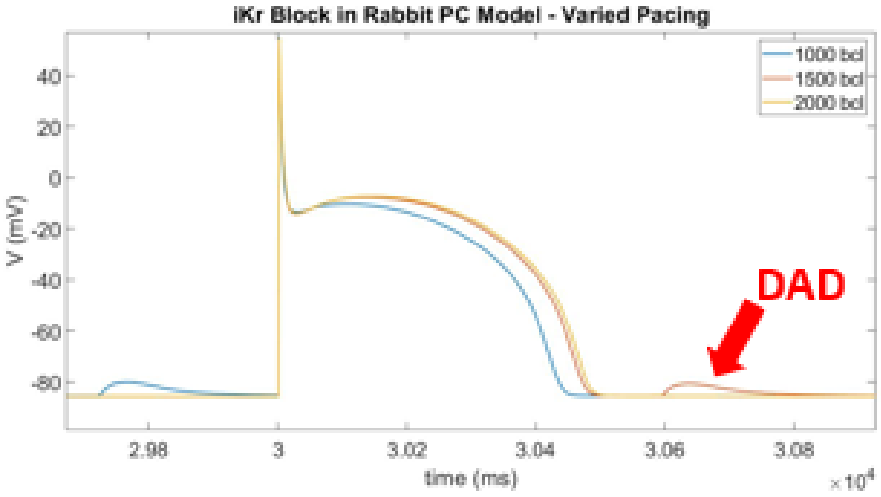
iKr Block in Rabbit PC Model - Varied Pacing
1000 bcl
1500 bcl
2000 bcl
DAD
V (mV)
time (ms)
×10^4

Fig. 10. Comparison of varied pacing in rabbit VM (A and B) and PC (C and D) model. PCs have a more pronounced APD prolongation.

A comparison of the original rabbit VM model and the SCR modified model reveals that the SCR model has a heightened propensity for ectopic beats with complete I_{Kr} blockage under isoproterenol conditions as shown in Fig. 11. The figure shows increased propensity for arrhythmogenic activity in the SCR rabbit model compared to the original UCLA_RAB model. Under the same conditions, which is complete I_{Kr} blockage and isoproterenol conditions, the SCR model exhibits spontaneous activity and creates ectopic beats.

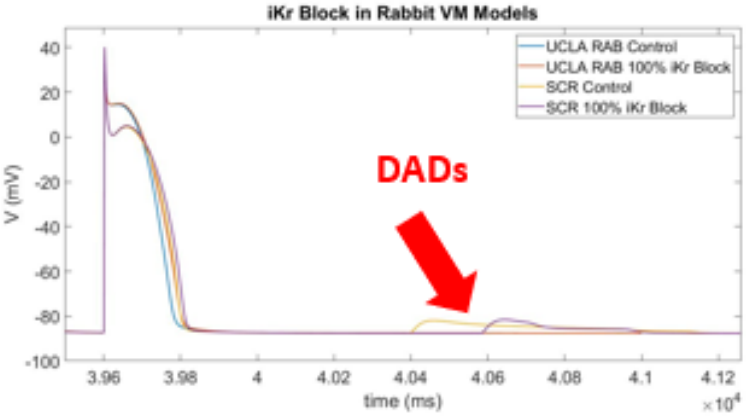

A.

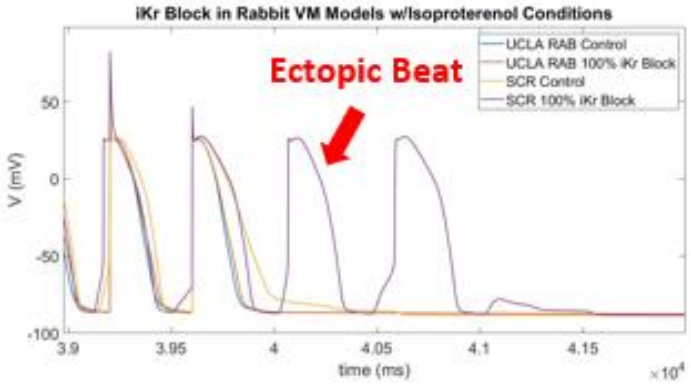

B.

Fig. 11. Comparison of APD prolongation and spontaneous activity produced in the VM and SCR rabbit models, indicating that the SCR model has a higher propensity for ectopic beats with complete I_{Kr} blockage under isoproterenol conditions.

HUMAN PURKINJE CELLS VERSUS VENTRICULAR MYOCYTES

In the human computational models, the control outputs from the VM and PC models, as shown in Fig. 12, confirm the experimentally reported AP morphologies in the two cell types. A comparison of the varied I_{Kr} blockage in VMs versus PCs reveals a more pronounced APD

prolongation in PCs. This enhanced prolongation in human cardiac cells is shown in Fig. 12 (B) and (C). Though no spontaneous activity is yet present, this APD prolongation can still be dangerous for the patient and may result in propagation of arrhythmia. Graph 2 represents an explanation for the more severe APD prolongation in PCs, as I_{Ks} has a greater amplitude in VM than in PCs. This potential mechanistic link will be investigated further in the discussion.

A.

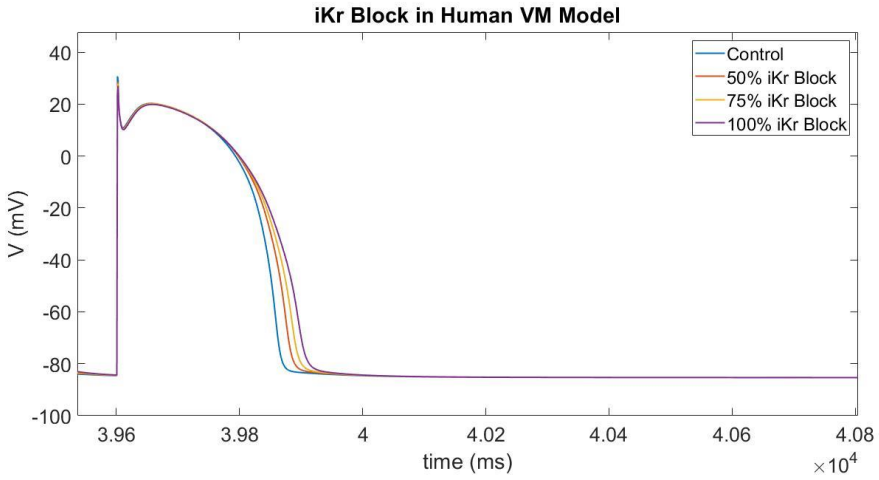

B.

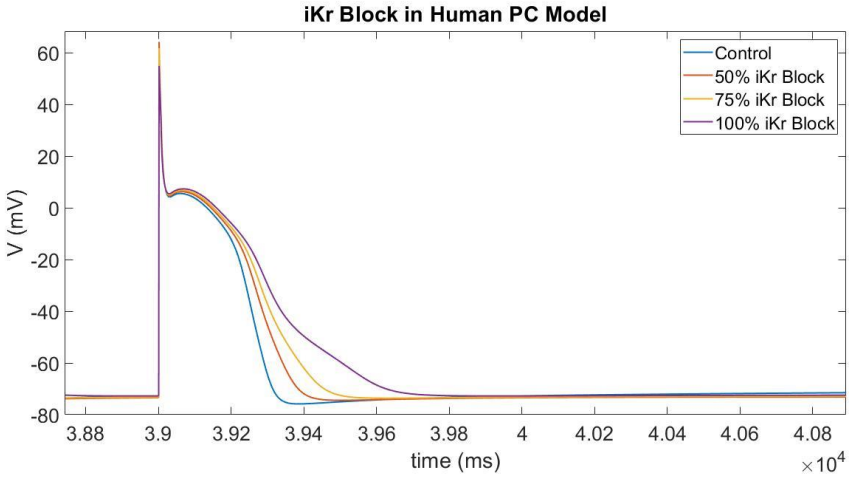

C.

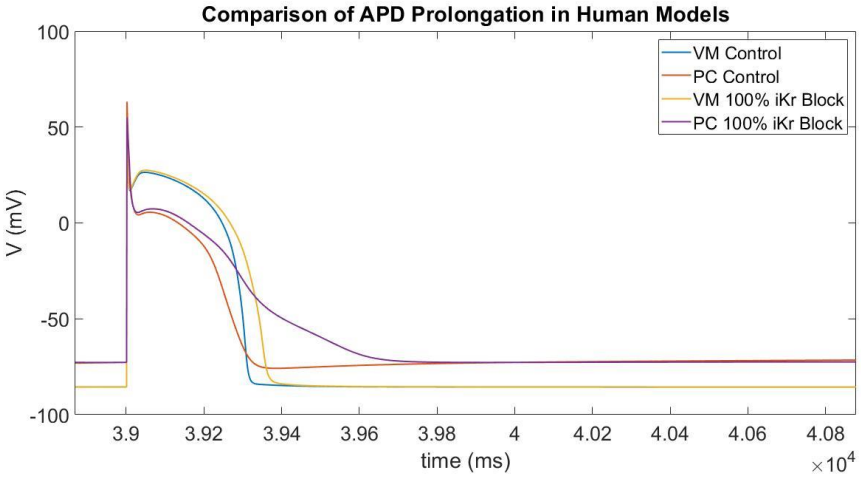

Fig. 12. Comparison of varied levels of I_{Kr} blockage in human VM (A) and PC (B) models. Comparison of 0 versus 100% I_{Kr} blockage in human VM and PC models (C). PCs have a more pronounced APD prolongation.

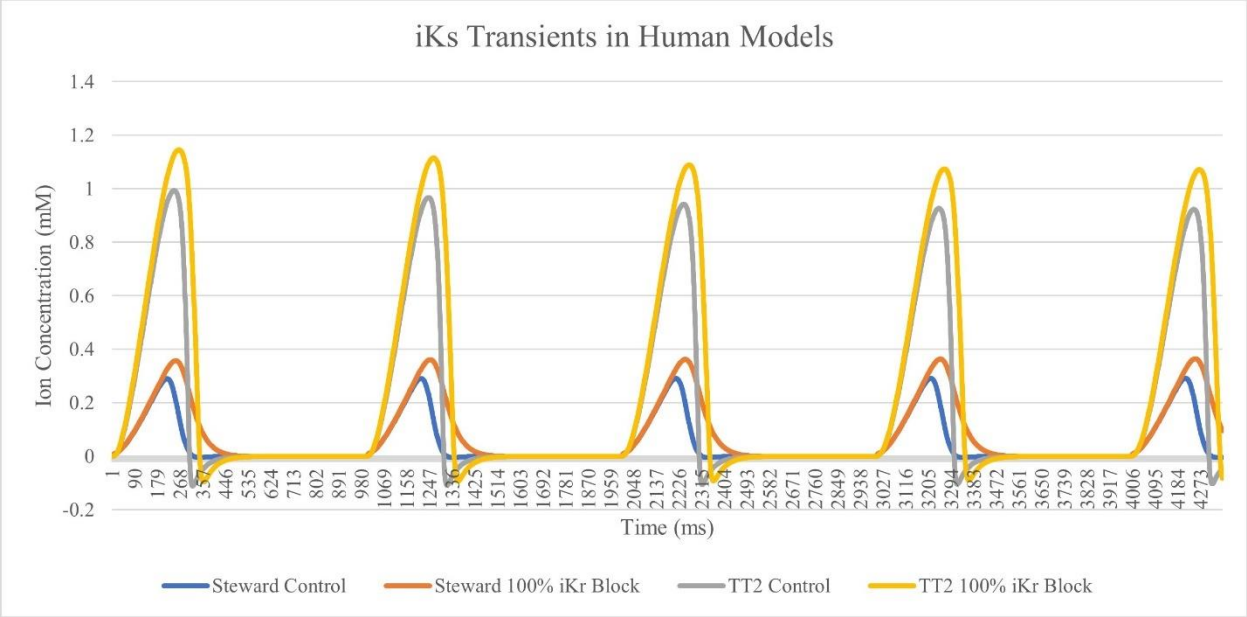

Graph 2. Plot of I_{Ks} transients over time for the human PC and VM models. This indicates that under I_{Ks} block conditions, I_{Ks} must compensate for the missing repolarizing current. VMs appear to have a greater increase in I_{Ks} transients with I_{Kr} blockage.

Under isoproterenol conditions, both the control and I_{Kr} block simulations did not produce any unwanted spontaneous activity. In the human PC model, however, both the control and I_{Kr} blockage produce spontaneous APs, or ectopic beats, as shown in Fig. 13. This will again be investigated further in the discussion.

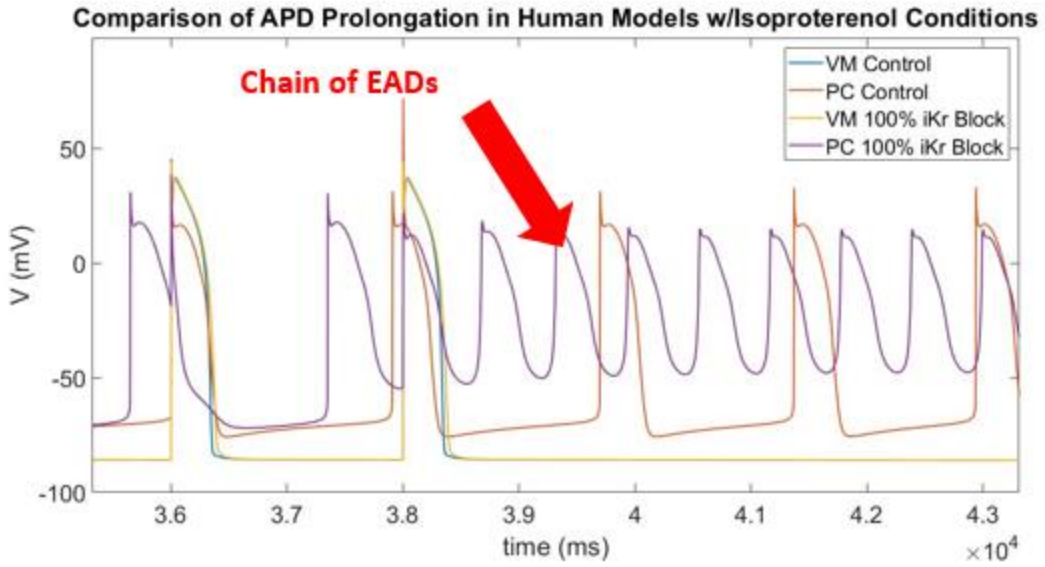

Fig. 13. Comparison of APD prolongation in human models with isoproterenol conditions and 100% I_{Kr} blockage showing ectopic beats in both control and I_{Kr} block conditions in the presence of isoproterenol.

DISCUSSION

LQT2 SEVERITY IN VM VERSUS PC

This study utilized single cell simulations involving rabbit and human cardiac cell models to explore arrhythmogenic mechanisms in LQT2 conditions. The principal findings of this study indicate that 1) a loss of I_{Kr} function in PCs produces a more severe phenotype than in VMs, 2) VMs have a greater magnitude of I_{Ks} in the absence of I_{Kr}, than that in PCs, 3) the SCR rabbit model has a heightened propensity for spontaneous activity, and 4) the computational models of human PCs have a heightened propensity for ectopic beats than human VMs as well as their counterparts in rabbit cells.

The results of this research are consistent with experimental findings reported in PCs and VMs. Specifically, both the rabbit and human biophysical models accurately depicted the spike and dome morphology of the cardiac AP. Both models were consistent with experimental findings regarding the voltage at which the plateau phase occurs and the resting membrane potential of the cells [23].

In both the rabbit and human simulations, PCs clearly have a more severe LQT2 phenotype than VMs as indicated by the higher percent increase in APD using both experimental and computational research methods. A likely explanation for this difference is a reduced repolarization reserve in PCs compared to VMs as indicated by the transient I_{Ks} currents shown in Graphs 1 and 2. This supports the hypothesis that the repolarization reserve in PCs is lower than that of VMs which leads to more severe phenotype in PCs. VMs exhibit higher amplitude of I_{Ks} which helps in part to compensate for the loss of I_{Kr} function. Therefore the effect of I_{Kr} blockade in VMs is relatively smaller when compared to PCs. Experimentally, it has been shown

that I_{Ks} plays a larger role in the APs of VMs than PCs [24]. I_{Ks} compensates for the loss of I_{Kr} in both cell types. In PCs, however, there is not as much I_{Ks} present, so the repolarization reserve is not as strong as it is in VMs, so it cannot compensate as much. This leads to more severe APD prolongation.

Analysis of the varied pacing in both VM and PCs suggests that even in the case of I_{Kr} blockage, higher frequency pacing results in shorter APDs. This is consistent with prior studies that establish lower APDs in higher frequency pacing of cardiac cells under control conditions [25]. It should also be noted that the SCR rabbit model showed a heightened propensity for spontaneous activity under both the control and I_{Kr} block conditions as shown in Campos et al.'s work [13]. This confirms that this model, when coupled with the rabbit PC, should allow for propagation of an arrhythmogenic beat through the PMJ, more accurately representing an LQT2 patient than current models are able to produce due to electrotonic loading [26].

The final discussion point is that isoproterenol conditions evoked spontaneous activity in both the control and the I_{Kr} blockage conditions in the human PC model. This can be explained by the fact that isoproterenol results in increased Ca^{2+} currents, based on experimental findings. This increase in Ca^{2+} results in the spontaneous APs shown in the previous slide. With I_{Kr} blockage, however, the cells are not even fully repolarizing. We're seeing a continuous chain of EADs. These EADs are dangerous because these oscillations can lead to triggering of premature ventricular beats, known as Torsade de Pointes (TdP). It has been well-established in prior literature of experiments that TdPs are closely related to PC activity [27].

RABBITS VERSUS HUMANS

The AP morphologies of PCs versus VMs have a more distinct difference in the human models compared to the rabbit models, as the human PC model more closely represents the characteristic spike and dome morphology of the cardiac AP. In isoproterenol conditions, the human PC models show a heightened sensitivity to the blockage of I_{Kr} as indicated by the presence of spontaneous APs compared to the rabbit PC model. The difference in this spontaneous activity likely relates to the relative influence of I_{Kr} in rabbits versus humans. I_{Kr} blockage results in a more extreme APD prolongation in humans than in dogs [28] and more in dogs than in rabbits [29], so it can be inferred that I_{Kr} blockage results in greater APD prolongation in humans. This abnormal repolarization can result in cardiac arrhythmias, which are indicated in simulations by ectopic beats as seen in the human PC model.

CONCLUSION

Experimental and computational findings were coupled to investigate and compare the arrhythmogenic potential under LQTS conditions in PCs and VMs in rabbits and humans. These models accurately reproduced experimental APD prolongation under I_{Kr} blockage and provided insight into the mechanisms behind the more severe LQTS phenotype in PCs. APD prolongation appeared to be more severe in PCs than VMs in both the experimental and computational components of this research. Spontaneous activity was not seen in VMs, but it was present in PCs in both the rabbit and human models, either as DADs, EADs, or full ectopic beats. The SCR model did successfully have spontaneous activity, so it may be useful in future applications. Under isoproterenol conditions, the human PC model showed spontaneous activity as well.

When working in computer simulations, dissociation from the subject matter is not difficult. These findings do have major clinical implications that need to be considered. In clinical or experimental studies, it is difficult to isolate individual factors causing fatal arrhythmias due to the coupling of parameters. With these findings, we have furthered our understanding of the specific mechanisms underlying LQTS and what's affecting these young patients.

RESEARCH LIMITATIONS

For the experimental component of the research, there were several limitations involving the preparation of the samples. Rabbit hearts are very small, typically measuring 2-3 inches long. When attempting to isolate the PC or VM with the electrode, it proved immensely difficult to get the tips of the electrodes on cells that were within close proximity of one another due to the size of the electrodes themselves. For example, this research initially sought to measure junctional characteristics and measure the time delay between PCs and the VMs that they were connected to, but that was not possible in this phase of experiments. Another difficulty that was experienced was the difficulty to determine which parts of the branching structure of the heart were Purkinje fibers versus just structural components of the heart that need to be clipped away. Additionally, each tissue-level experiment took an entire day, usually up to 12 hours, to complete. Because the lab was being utilized for other projects as well, it became difficult to repeat the same procedure with multiple rabbits. The final experimental limitation was that isoproterenol was not able to be used due to time restrictions.

The main limitation with the computational component of this research is that these simulations were all run in single cells. The effects were not measured in multicell simulations to determine the transfer of arrhythmogenic potential from one cell to another or to investigate the propagation of arrythmias from PC to VMs through PMJs. Another limitation in the simulations is the electrotonic loading effect in 3-dimensional models. Again, this project originally sought to investigate the propagation of arrythmias from PCs to VMs through the PMJs, but the electrotonic loading created from one PC connecting to many VMs tends to suppress the spontaneous activity in the simulations. The final computational limitation was the inability to maintain a constant pacing throughout all simulations due to the extreme APD prolongation under certain conditions, such as complete I_{Kr} blockage and isoproterenol in the human PC. In this case, the AP took so long to repolarize that a BCL of 2,000 ms was required to allow for complete repolarization. All rabbit simulations were completed at a BCL of 400 ms to replicate the findings of prior studies [13].

SUGGESTIONS FOR FUTURE RESEARCH

To reiterate, the experimental results were very limited in terms of the number of experiments completed, the experimental groups, and the consistency of distance between electrodes. Future experiments should include a standard distance between the electrodes, one that allows the junctional characteristics and mechanisms for arrhythmia propagation to be measured if at all feasible. Isoproterenol effects should be included in experiments to compare the APD prolongation under stress conditions in the tissue.

Additionally, LQT2 effects were drug-induced by E-4031, the I_{Kr} blocker, not by the actual *hERG* gene mutation. Transfection of the patients' gene mutation into the cells should be done in future work to investigate the mutation itself and to help determine what level of E-4031 properly relates to the gene mutation. A clear avenue for future research is to implement the changes made in the SCR rabbit model to the human VM model to create a myocardium more susceptible to propagation of arrhythmia. Coupled with the human PC model, the SCR model may overcome the electronic loading effect, which will allow further investigation in the propagation of arrhythmogenic activity through PMJs. Further investigation of PMJs can be done on the time delay from PCs to VMs. Once the control output matches physiological standards, these models can be modified to determine the exact mechanisms underlying the propagation of spontaneous activity like DADs and EADs propagate through the myocardium, potentially resulting in reentry circuits. By investigating these findings in 3D, we will be even closer to understanding the exact mechanism of LQTS that causes arrythmia, which can help in treatment of the condition.

REFERENCES

[1] S. G. Priori, R. Bloise, and L. Crotti, "The long QT syndrome," *Europace*, vol. 3, no. 1, pp. 16-27, Jan 2001, doi: 10.1053/eupc.2000.0141.

[2] L. Carlsson, C. Abrahamsson, L. Drews, G. Duker. “Antiarrhythmic effects of potassium channel openers in rhythm abnormalities related to delayed repolarization,” *Circulation*, vol. 85, no. 4, pp. 1491-1500, Apr 1992, doi: 10.1161/01.CIR.85.4.1491.

[3] D. Sedmera and R. G. Gourdie, "Why do we have Purkinje fibers deep in our heart?," *Physiol Res*, vol. 63, no. Suppl 1, pp. S9-18, 2014, doi: 10.33549/physiolres.932686.

[4] J. Jalife, M. Delmar, A. Justus, B. Omer, and J. Kalifa, “Basic Cardiac Electrophysiology for the Clinician,” Blackwell Publishing, Chichester, United Kingdom, pp. 7-42, 2009.

[5] V. Garcia-Bustos, R. Sebastian, M. Izquierdo, P. Molina, F. J. Chorro, and A. Ruiz-Sauri, "A quantitative structural and morphometric analysis of the Purkinje network and the Purkinje-myocardial junctions in pig hearts," *J Anat*, vol. 230, no. 5, pp. 664-678, May 2017, doi: 10.1111/joa.12594.

[6] V. Olejnickova et al., "Gap Junctional Communication via Connexin43 between Purkinje Fibers and Working Myocytes Explains the Epicardial Activation Pattern in the Postnatal Mouse Left Ventricle," *Int J Mol Sci*, vol. 22, no. 5, Mar 2021, doi: 10.3390/ijms22052475.

[7] G. Malfatto, G. Beria, S. Sala, O. Bonazzi, and P. J. Schwartz. “Quantitative analysis of T wave abnormalities and their prognostic implications in the idiopathic long QT syndrome,” *J Am Coll Cardiol*, vol. 23, no. 2, pp. 296-301, Feb 1994.

[8] H. Lu, E Vlaminckx, K. Van Ammel, and F. De Clerck, “Drug-induced long QT in isolated rabbit Purkinje fibers: importance of action potential duration, triangulation and early afterdepolarizations,” *Eur J Pharmacol*, vol. 452, no. 2, Oct 2002, doi: 10.1016/s0014-2999(02)02246-x.

[9] R. Dumaine and J. M. Cordeiro, “Comparison of K+ currents in cardiac Purkinje cells isolated from rabbit and dog,” *J Mol Cell Cardiol*, vol. 42, no. 2, pp. 378-389, Feb 2007, doi:10.1016/j.yjmcc.2006.10.019.

[10] Y. Rudy and J. R. Silva, "Computational biology in the study of cardiac ion channels and cell electrophysiology," *Q Rev Biophys*, vol. 39, no. 1, pp. 57-116, 2006, doi: 10.1017/S0033583506004227.

[11] T. O'Hara and Y. Rudy, "Quantitative comparison of cardiac ventricular myocyte electrophysiology and response to drugs in human and nonhuman species," *Am J Physiol Heart Circ Physiol*, vol. 302, no. 5, pp. H1023-30, Mar 1 2012, doi: 10.1152/ajpheart.00785.2011.

[12] D. G. Whittaker, M. Clerx, C. L. Lei, D. J. Christini, and G. R. Mirams, "Calibration of ionic and cellular cardiac electrophysiology models," *Wiley Interdiscip Rev Syst Biol Med*, vol. 12, no. 4, p. e1482, Jul 2020, doi: 10.1002/wsbm.1482.

[13] F. O. Campos, Y. Shiferaw, A. J. Prassl, P. M. Boyle, E. J. Vigmond, and G. Plank, "Stochastic spontaneous calcium release events trigger premature ventricular complexes by overcoming electrotonic load," *Cardiovasc Res*, vol. 107, no. 1, pp. 175-83, Jul 1 2015, doi: 10.1093/cvr/cvv149.

[14] W. Chen, G. Aistrup, J. A. Wasserstrom, and Y. Shiferaw, “A mathematical model of spontaneous calcium release in cardiac myocytes,” *Am J Physiol Heart Circ Physiol*, vol. 300, no. 5, pp. H1794-H1805, May 2011, doi: 10.1152/ajpheart.01121.2010.

[15] C. Lengyel et al. "Pharmacological block of the slow component of the outward delayed rectifier current (IKs) fails to lengthen rabbit ventricular muscle QTc and action potential duration," *British journal of pharmacology*, vol. 132, no. 1, pp. 101-110, 2001.

[16] A. Mahajan et al., “A rabbit ventricular action potential model replicating cardiac dynamics at rapid heart rates,” *Biophys. J.*, vol. 94, no. 2, pp. 392–410, 2008, doi: 10.1529/biophysj.106.98160.

[17] O. V. Aslanidi, R. N. Sleiman, M. R. Boyett, J. C. Hancox, and H. Zhang, “Ionic mechanisms for electrical heterogeneity between rabbit purkinje fiber and ventricular cells,” *Biophys. J.*, vol. 98, no. 11, pp. 2420–2431, 2010, doi: 10.1016/j.bpj.2010.02.033.

[18] T. R. Shannon, F. Wang, J. Pugliisi, C. Weber, and D. M. Bers, “A mathematical treatment of integrated Ca dynamics within the ventricular myocyte,” *Biophys. J.*, vol. 87, no. 5, pp. 3351-3371, Nov 2004, doi: 10.1529/biophysj.104.047449.

[19] K. H. ten Tusscher, D. Noble, P. J. Noble, and A. V. Panfilov, “A human model for human ventricular tissue,” *Am J Physiol Heart Circ Physiol*, vol. 286, no. 4, pp. H1573-H1589, Apr 2004, doi: 10.1152/ajpheart.00794.2003.

[20] P. Stewart, O. V. Aslanidi, D. Noble, P. J. Noble, M. R. Boyett, and H. Zhang, “Mathematical models of the electrical action potential of Purkinje fibre cells,” *Philosophical Transactions of the Royal Society A: Mathematical, Physical and Engineering Sciences*, vol. 367, no. 1896, pp. 2225-2255, Jun 2009, doi: 10.1098/rsta.2008.0283.

[21] A. Prassl et al., "- User's Manual - Anton Prassl," 2020.

[22] C. Shah, S. Jiwani, B. Limbu, S. Weinberg, and M. Deo, "Delayed afterdepolarization-induced triggered activity in cardiac purkinje cells mediated through cytosolic calcium diffusion waves," *Physiological reports*, vol. 7, no. 24, pp. 1-14, Dec 2019, doi: 10.14814/phy2.14296.

[23] J. M. Cordeiro, K. W. Spitzer, and W. R. Giles, "Repolarizing K+ currents in rabbit heart Purkinje cells," *The Journal of Physiology*, vol. 508, no. 3, pp. 811-823, May 1998.

[24] J. M. Nerbonne, "Molecular basis of functional voltage-gated K+ channel diversity in the mammalian myocardium," *The Journal of physiology*, vol. 525, no. 2, pp. 285-298, Jun 2000.

[25] J. M. Morgan, A. D. Cunningham, and E. Rowland, "Relationship of the Effective Refractory Period and Monophasic Action Potential Duration after a Step Increase in Pacing Frequency," *Pacing and Clinical Electrophysiology*, vol. 13, no. 8, pp. 1002-1008, Aug 1990, doi: 10.1111/j.1540-8159.1990.tb02147.x.

[26] A. D. Akwaboah et al., "An in silico hiPSC-Derived Cardiomyocyte Model Built With Genetic Algorithm," *Front. Physiol.*, vol. 12, pp. 1–24, 2021, doi: 10.3389/fphys.2021.675867.

[27] C. Lengyel, A. Varró, K. Tábori, J. Papp, and I. Baczkó, "Combined pharmacological block of IKr and IKs increases short-term QT interval variability and provokes torsades de pointes," *British journal of pharmacology*, vol. 151, no. 7, pp. 941-951, Aug, 2007, doi: 10.1038/sj.bjp.0707297.

[28] N. Jost et al., “Ionic mechanisms limiting cardiac repolarization reserve in humans compared to dogs,” *The Journal of physiology*, vol. 591, no. 17, pp. 4189-4206, Sep 2013, doi: 10.1113/jphysiol.2013.261198.

[29] N. El-Sherif, R. H. Zeiler, W. Craelius, W. B. Gough, and R. Henkin, “QTU prolongation and polymorphic ventricular tachyarrhythmias due to bradycardia-dependent early afterdepolarizations. Afterdepolarizations and ventricular arrhythmias.,” *Circ Res*, vol. 64, no. 2, pp. 286-305, Aug 1988.

VITA

Victoria Lin Lam is pursuing a Master of Science in Engineering and Technology at Old Dominion University, located in Norfolk, Virginia. ODU's Batten College of Engineering & Technology is located at 1105 Engineering Systems Building, Norfolk, VA 23529. Before attending ODU, she earned a Bachelor of Science in Neuroscience at the College of William and Mary in Williamsburg, Virginia in May of 2019. Her professional experience includes working as a research assistant for ODU who partners with Norfolk State University for their NIH-funded project on cardiac modeling of LQTS. While earning her M.S., Victoria was inducted into Omicron Delta Kappa Honor Society and the Society for Collegiate Leadership and Achievement for exceptional leadership and academic achievement during her graduate studies.